

# ATS643LSH

## Self-Calibrating, Zero-Speed Differential Gear Tooth Sensor with Continuous Update

Package SH, 4-pin SIP



1. VCC
2. No connection (float or tie to VCC)
3. Test pin (float or tie to GND)
4. GND

### ABSOLUTE MAXIMUM RATINGS

Supply Voltage, $V_{CC}$	See Power Derating
Reverse-Supply Voltage, $V_{RCC}$	-18 V
Operating Temperature	
Ambient, $T_A$	-40°C to 150°C
Maximum Junction, $T_{J(max)}$	165°C
Storage Temperature, $T_S$	-65°C to 170°C

The ATS643 is an optimized combination of integrated circuit and magnet that provides a manufacturer-friendly solution for true zero-speed digital gear-tooth sensing in two-wire applications. The device consists of a single-shot molded plastic package that includes a samarium cobalt magnet, a pole piece, and a Hall-effect IC that has been optimized to the magnetic circuit and the automotive environment. This small package can be easily assembled and used in conjunction with a wide variety of gear shapes and sizes.

The integrated circuit incorporates a dual element Hall-effect sensor with signal processing circuitry that switches in response to differential magnetic signals created by rotating ferrous targets. The device contains a sophisticated compensating circuit to eliminate magnet and system offsets immediately at power-on. Digital tracking of the analog signal is used to achieve true zero-speed operation, while also setting the device switchpoints. The resulting switchpoints are air gap independent, greatly improving output and duty cycle accuracy. The device also uses a continuous update algorithm to fine-tune the switchpoints while in running mode, maintaining the device specifications even through large changes in air gap or temperature.

The regulated current output is configured for two-wire operation, offering inherent diagnostic information. This device is ideal for obtaining speed and duty cycle information in gear-tooth based applications such as transmission speed sensing.

### Features and Benefits

- Fully-optimized differential digital gear tooth sensor
- Single chip-IC for high reliability
- Internal current regulator for 2-wire operation
- Small mechanical size (8 mm diameter x 5.5 mm depth)
- Switchpoints air gap independent
- Digital output representing gear profile
- Precise duty cycle accuracy throughout temperature range
- Large operating air gaps
- <2 ms power-on time
- AGC and reference adjust circuit
- True zero-speed operation
- Undervoltage lockout
- Wide operating voltage range
- Defined power-on state

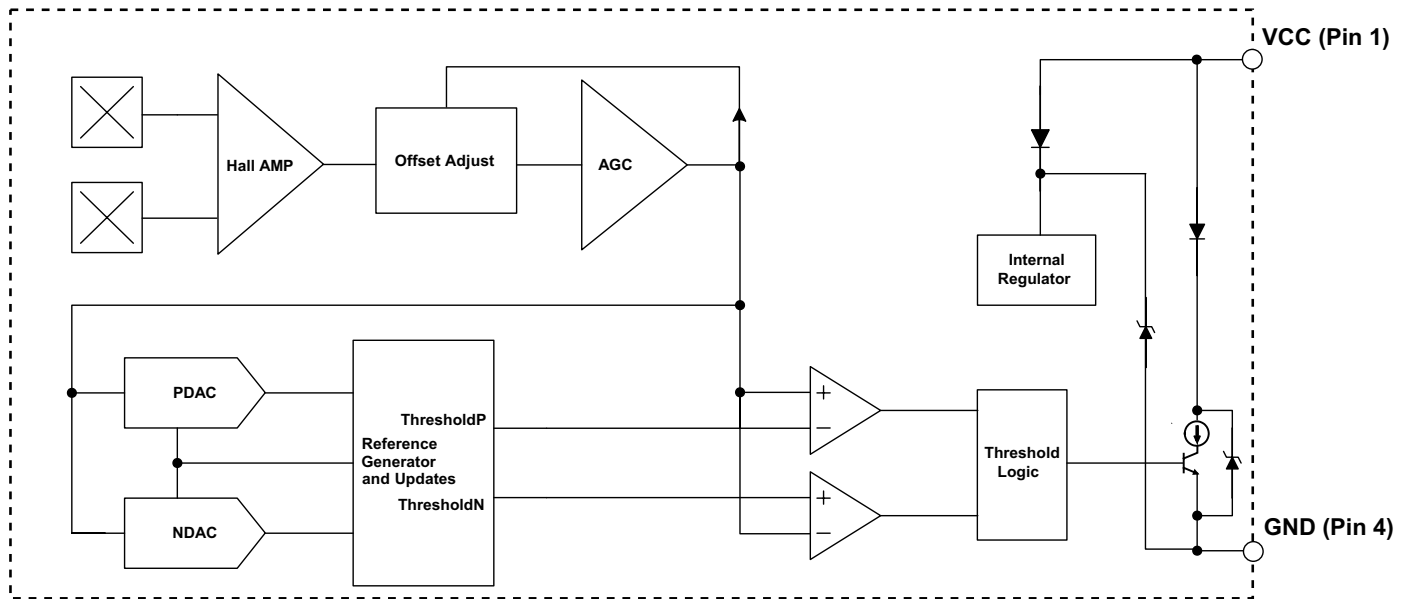
Use the following complete part numbers when ordering:

Part Number	Package	$I_{CC}$ Typical
ATS643LSH-I1	4-pin plastic SIP	6.0 Low to 14.0 High mA
ATS643LSH-I2	4-pin plastic SIP	7.0 Low to 14.0 High mA

# ATS643LSH

Self-Calibrating, Zero-Speed Differential GTS with Continuous Update

## Functional Block Diagram



# ATS643LSH

Self-Calibrating, Zero-Speed Differential GTS with Continuous Update

OPERATING CHARACTERISTICS using reference target 60-0, T <sub>A</sub> and V <sub>CC</sub> within specification, unless otherwise noted						
Characteristic	Symbol	Test Conditions	Min.	Typ.	Max.	Units
<b>ELECTRICAL CHARACTERISTICS</b>						
Supply Voltage	V <sub>CC</sub>	Operating; T <sub>J</sub> < 165 °C	4.0	–	24	V
Undervoltage Lockout	V <sub>CC(UV)</sub>	V <sub>CC</sub> 0 → 5 V	–	3.5	4.0	V
Supply Zener Clamp Voltage	V <sub>Z</sub>	I <sub>CC</sub> = 19 mA for ATS643-I1, and 19.8 mA for ATS643-I2; T <sub>A</sub> = 25°C	28	–	–	V
Supply Current	I <sub>CC(Low)</sub>	ATS643-I1	4.0	6	8.0	mA
		ATS643-I2	5.9	7	8.4	mA
	I <sub>CC(High)</sub>	ATS643-I1	12.0	14.0	16.0	mA
		ATS643-I2	11.8	14.0	16.8	mA
Supply Current Ratio	I <sub>CC(High)</sub> /I <sub>CC(Low)</sub>	Ratio of high current to low current	1.85	–	3.05	–
<b>POWER-ON CHARACTERISTICS</b>						
Power-On State	I <sub>CC(PO)</sub>	t < t <sub>on</sub> ; dI/dt < 5 μs	–	High	–	mA
Power-On Time <sup>1</sup>	t <sub>on</sub>	Target gear speed < 100 rpm	–	1	2	ms
<b>OUTPUT STAGE</b>						
Output Slew Rate <sup>2</sup>	dI/dt	R <sub>LOAD</sub> = 100 Ω, C <sub>LOAD</sub> = 10 pF	–	7	–	mA/μs
Output State	V <sub>OUT</sub>	R <sub>SENSE</sub> on high side (VCC pin); I <sub>CC</sub> = I <sub>CC(High)</sub>	–	Low	–	mV
		R <sub>SENSE</sub> on low side (GND pin); I <sub>CC</sub> = I <sub>CC(High)</sub>	–	High	–	mV

Continued on the next page.

# ATS643LSH

## Self-Calibrating, Zero-Speed Differential GTS with Continuous Update

<b>OPERATING CHARACTERISTICS</b> (continued) using reference target 60-0, $T_A$ and $V_{CC}$ within specification, unless otherwise noted						
Characteristic	Symbol	Test Conditions	Min.	Typ.	Max.	Units
<b>SWITCHPOINT CHARACTERISTICS</b>						
Rotation Speed	$S_{ROT}$	Reference Target 60-0	0	–	12,000	rpm
Bandwidth	BW	Equivalent to $f - 3dB$	25	40	–	kHz
<b>CALIBRATION</b> <sup>3</sup>						
Initial Calibration Period	$C_I$	Quantity of rising output (current) edges required for accurate edge detection	–	–	3	Edge
AGC Calibration Disable	$C_f$	Quantity of rising output (current) edges used for calibrating AGC	–	–	3	Edge
Start Mode Hysteresis	$PO_{HYS}$		–	175	–	mV
<b>DAC CHARACTERISTICS</b>						
Dynamic Offset Cancellation			–	±60	–	G
Tracking Data Resolution		Quantity of bits available for PDAC/NDAC tracking of both positive and negative signal peaks	–	9	–	Bit
<b>FUNCTIONAL CHARACTERISTICS</b>						
Air Gap Range <sup>4</sup>	AG	ADC within specification	0.5	–	2.5	mm
Maximum Operable Air Gap	$AG_{(opmax)}$	Output switching (no missed edges); ADC not guaranteed	–	–	2.75	mm
Duty Cycle Variation	$\Delta DC$	Wobble < 0.5 mm, AG within specification	–	–	±10	%
Input Signal Range	Sig	ADC within specification	40	–	1400	G
Minimum Operable Input Signal	$Sig_{(opmin)}$	Output switching (no missed edges); ADC not guaranteed	30	–	–	G

<sup>1</sup>Power-On Time includes the time required to complete the internal automatic offset adjust. The DACs are then ready for peak acquisition.

<sup>2</sup>dl is the difference between 10% of  $I_{CC(Low)}$  and 90% of  $I_{CC(High)}$ , and dt is time period between those two points. Note: dl/dt is dependent upon the value of the bypass capacitor, if one is used.

<sup>3</sup>Continuous Update (calibration) functions continuously during Running mode operation.

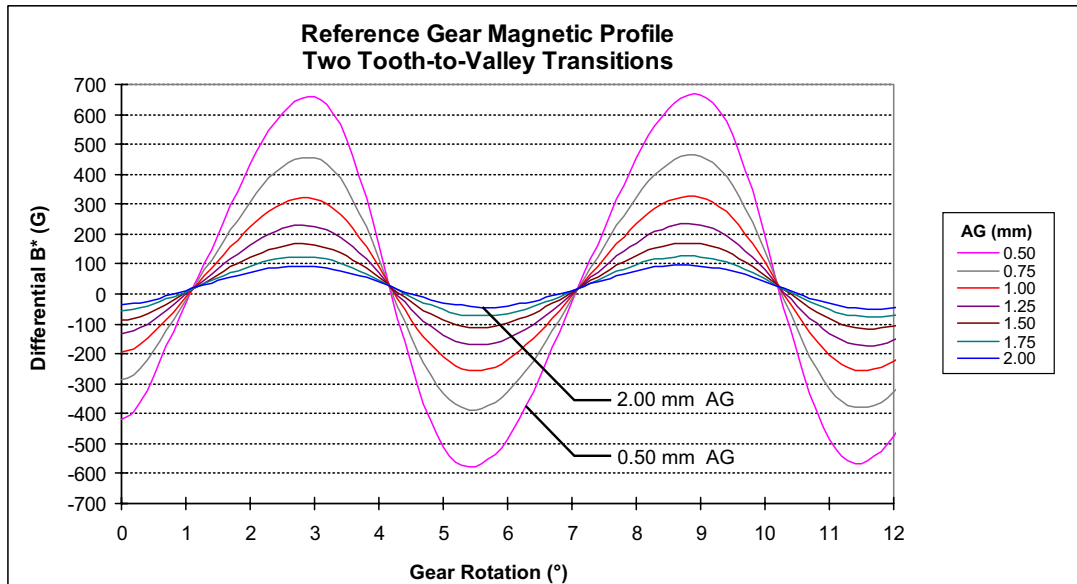
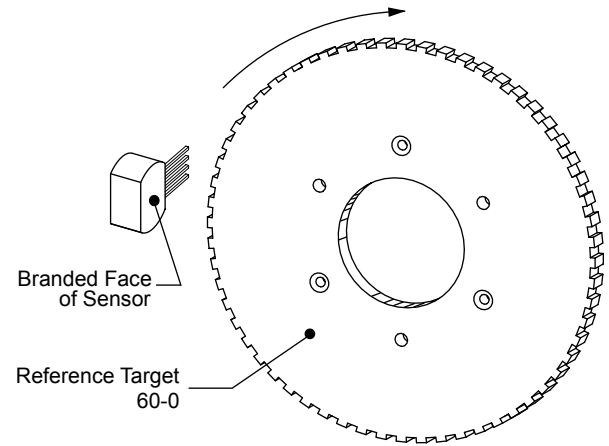
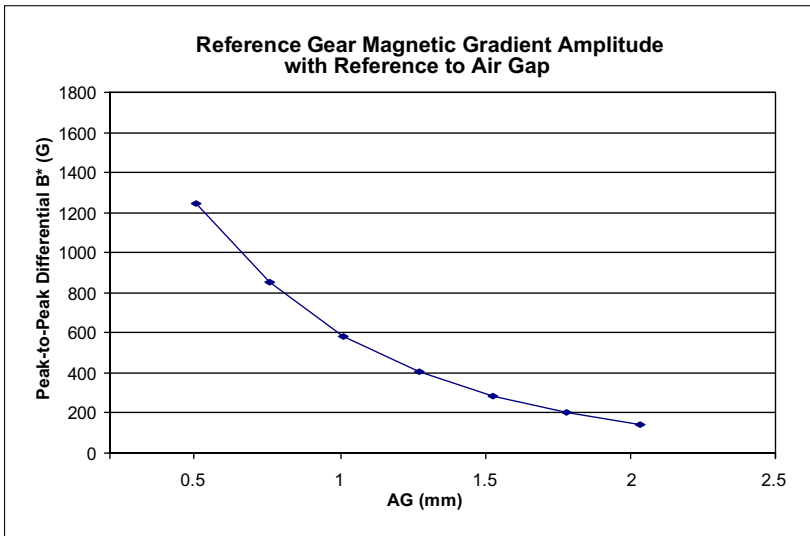
<sup>4</sup>AG is dependent on the available magnetic field. The available field is dependent on target geometry and material, and should be independently characterized. The field available from the reference target is given in the reference target parameter section of the datasheet.

# ATS643LSH

## Self-Calibrating, Zero-Speed Differential GTS with Continuous Update

### REFERENCE TARGET, 60-0 (60 Tooth Target)

Characteristics	Symbol	Test Conditions	Typ.	Units	Symbol Key
Outside Diameter	$D_o$	Outside diameter of target	120	mm	
Face Width	F	Breadth of tooth, with respect to sensor	6	mm	
Circular Tooth Length	t	Length of tooth, with respect to sensor; measured at $D_o$	3	mm	
Circular Valley Length	$t_v$	Length of valley, with respect to sensor; measured at $D_o$	3	mm	
Tooth Whole Depth	$h_t$		3	mm	
Material		Low Carbon Steel	—	—	



\*Differential B corresponds to the calculated difference in the magnetic field as sensed simultaneously at the two Hall elements in the device ( $B_{DIFF} = B_{E1} - B_{E2}$ ).

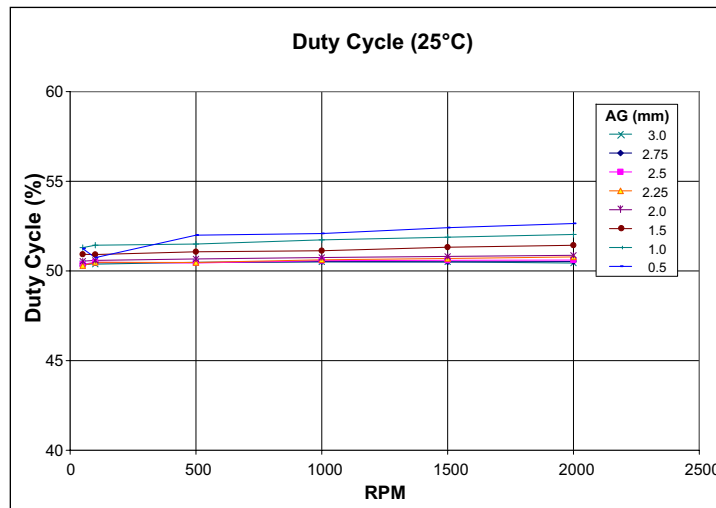
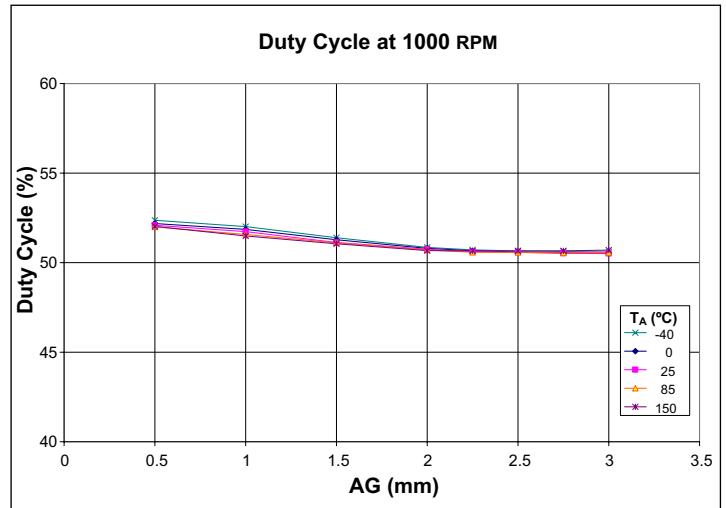
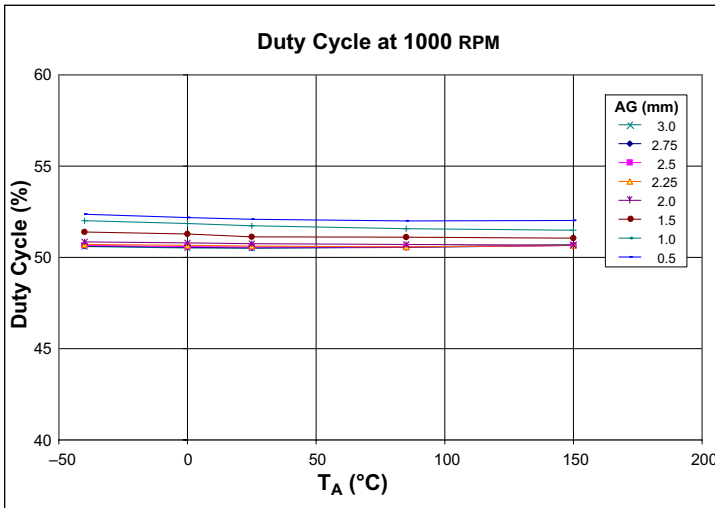
# ATS643LSH

Self-Calibrating, Zero-Speed Differential GTS with Continuous Update

## Characteristic Data

Data taken from 3 lots, 30 pieces/lot; 11 trim

Reference Target 60-0



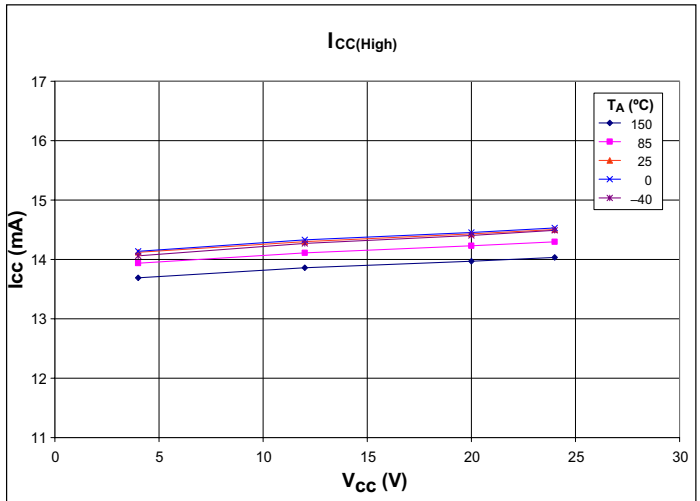
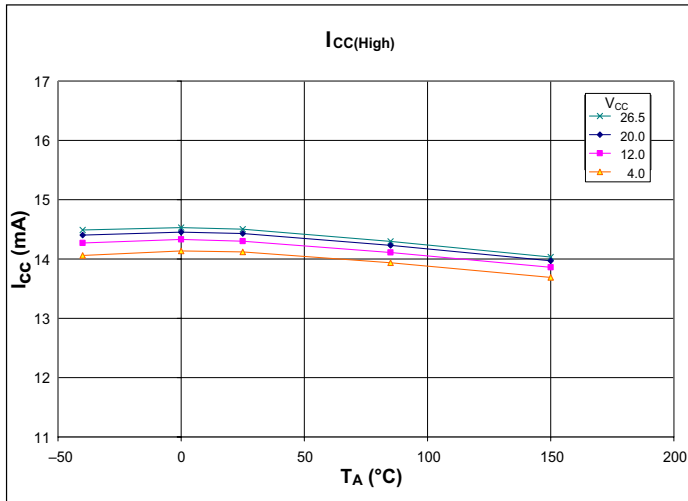
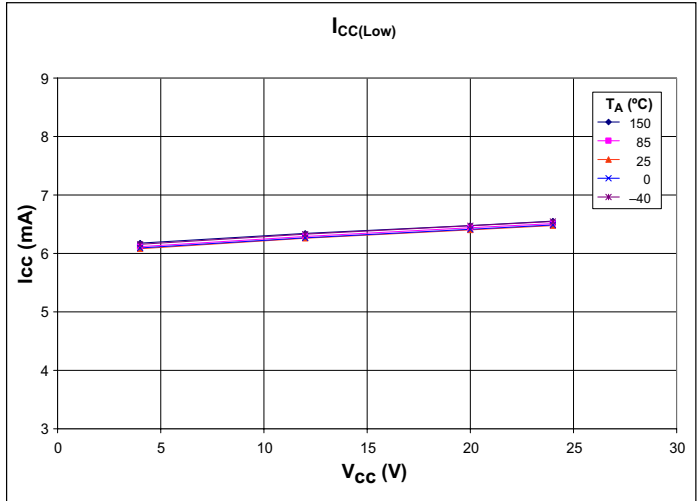
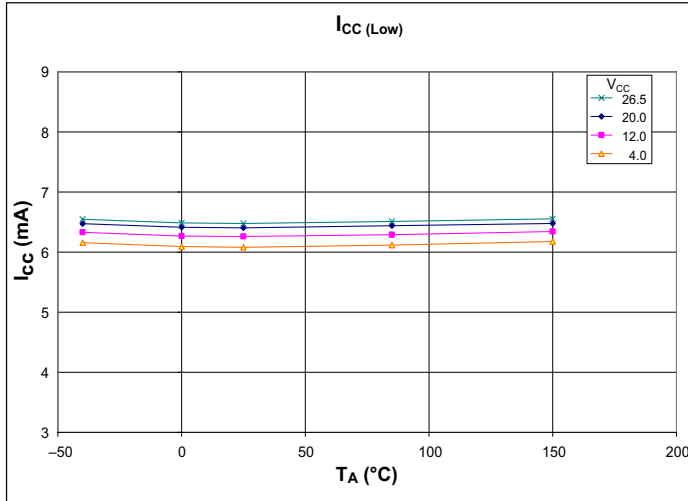
Continued on the next page.

# ATS643LSH

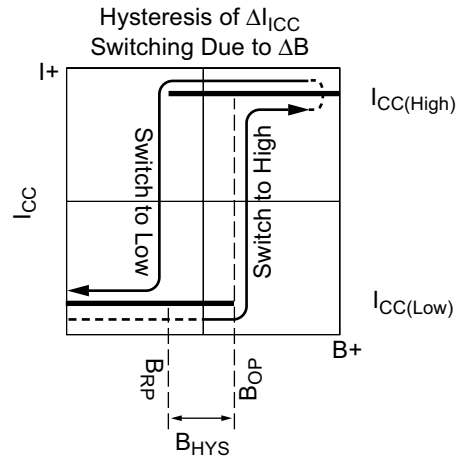
## Self-Calibrating, Zero-Speed Differential GTS with Continuous Update

### Characteristic Data (continued)

Data taken from 3 lots, 30 pieces/lot; I1 trim



Output current in relation to sensed magnetic flux density. Transition through  $B_{OP}$  must precede by transition through  $B_{RP}$ .

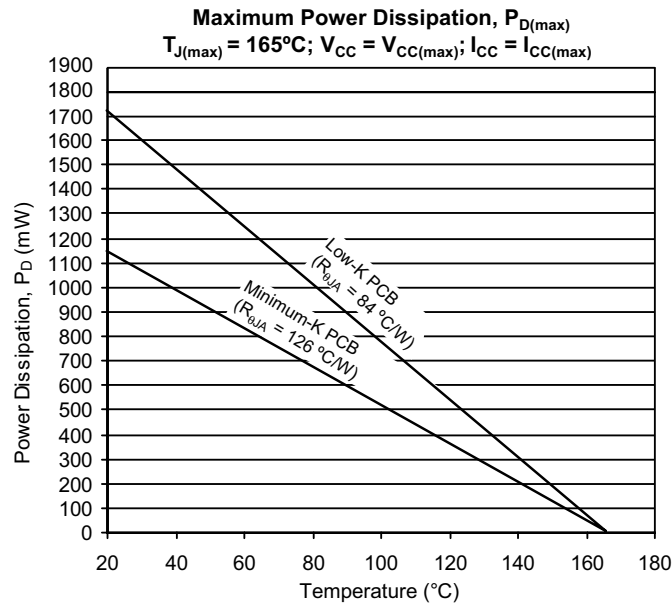
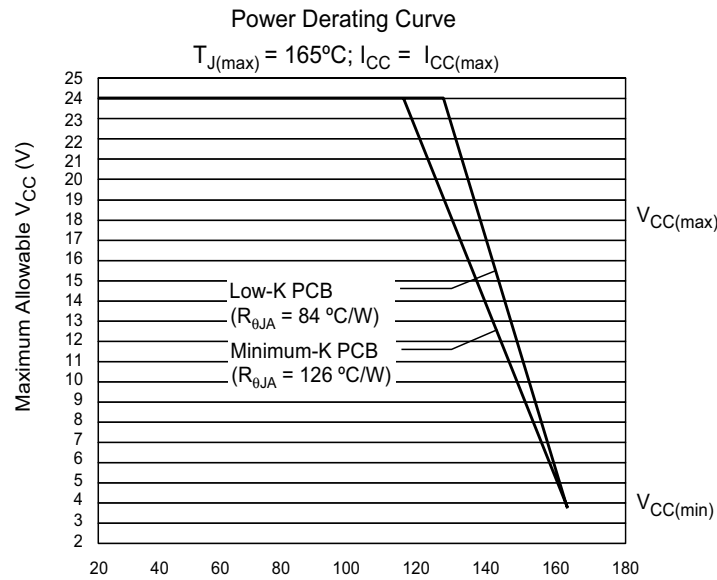


# ATS643LSH

Self-Calibrating, Zero-Speed Differential GTS with Continuous Update

**THERMAL CHARACTERISTICS** may require derating at maximum conditions, see application information

Characteristic	Symbol	Test Conditions	Min.	Typ.	Max	Units
Package Thermal Resistance	$R_{\theta JA}$	Minimum-K PCB (single-sided with copper limited to solder pads)	126	–	–	°C/W
		Low-K PCB (single-sided with copper limited to solder pads and 3.57 in. <sup>2</sup> (23.03 cm <sup>2</sup> ) of copper area)	84	–	–	°C/W





# ATS643LSH

## Self-Calibrating, Zero-Speed Differential GTS with Continuous Update

### Functional Description

**Sensing Technology.** The ATS643 module contains a single-chip differential Hall effect sensor IC, a samarium cobalt magnet, and a flat ferrous pole piece (concentrator). As shown in figure 1, the Hall IC supports two Hall elements, which sense the magnetic profile of the ferrous gear target simultaneously, but at different points (spaced at a 2.2 mm pitch), generating a differential internal analog voltage ( $V_{PROC}$ ) that is processed for precise switching of the digital output signal.

The Hall IC is self-calibrating and also possesses a temperature compensated amplifier and offset cancellation circuitry. Its voltage regulator provides supply noise rejection throughout the operating voltage range. Changes in temperature do not greatly affect this device due to the stable amplifier design and the offset rejection circuitry. The Hall transducers and signal processing electronics are integrated on the same silicon substrate, using a proprietary BiCMOS process.

**Target Profiling During Operation.** When proper power is applied to the sensor, it is capable of providing digital information that is representative of the mechanical features of a rotating gear. The waveform diagram in figure 3 presents the automatic translation of the mechanical profile, through the magnetic profile that it induces, to the digital output signal of the ATS643. No additional optimization is needed and minimal processing circuitry is required. This ease of use reduces design time and

incremental assembly costs for most applications.

**Determining Output Signal Polarity.** In figure 3, the top panel, labeled *Mechanical Position*, represents the mechanical features of the target gear and orientation to the device. The bottom panel, labeled *Sensor Output Signal*, displays the square waveform corresponding to the digital output signal that results from a rotating gear configured as shown in figure 2. That direction of rotation (of the gear side adjacent to the face of the sensor) is: perpendicular to the leads, across the face of the device, from the pin 1 side to the pin 4 side. This results in the sensor output switching from low,  $I_{CC(Low)}$ , to high,  $I_{CC(High)}$ , as the leading edge of a tooth (a rising mechanical edge, as detected by the sensor) passes the sensor face. In this configuration, the device output current switches to its high polarity when a tooth is the target feature nearest to the sensor. If the direction of rotation is reversed, so that the gear rotates from the pin 4 side to the pin 1 side, then the output polarity inverts. That is, the output signal goes high when a falling edge is detected, and a valley is the nearest to the sensor. Note, however, that the polarity of  $I_{OUT}$  depends on the position of the sense resistor,  $R_{SENSE}$  (see Operating Characteristics table).

**Continuous Update of Switchpoints.** Switchpoints are the threshold levels of the differential internal analog signal,  $V_{PROC}$ , at which the device changes output signal polarity. The value of

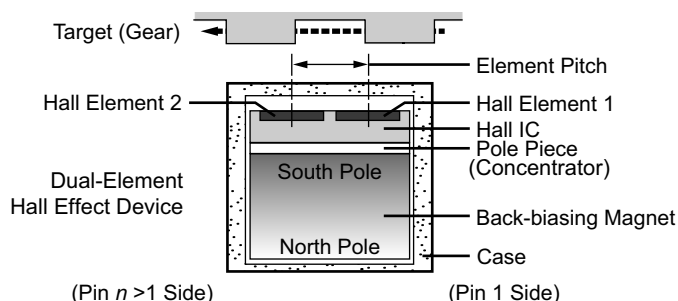


Figure 1. Relative motion of the target is detected by the dual Hall elements mounted on the Hall IC.

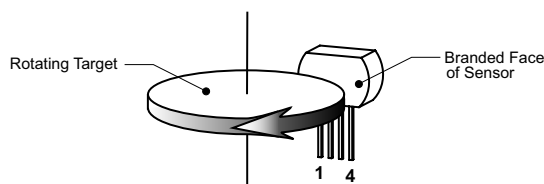


Figure 2. This left-to-right (pin 1 to pin 4) direction of target rotation results in a high output signal when a tooth of the target gear is nearest the face of the sensor (see figure 3). A right-to-left (pin 4 to pin 1) rotation inverts the output signal polarity.

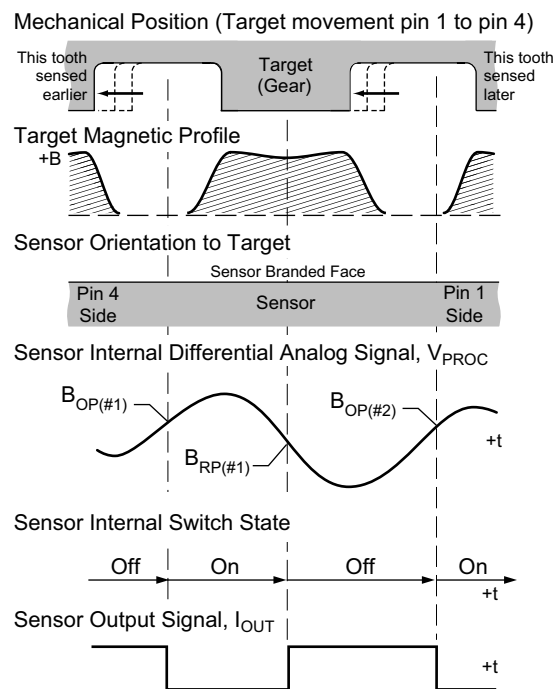


Figure 3. The magnetic profile reflects the geometry of the target, allowing the ATS643 to present an accurate digital output response.

# ATS643LSH

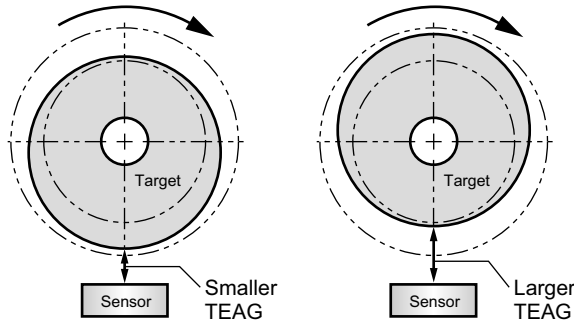
## Self-Calibrating, Zero-Speed Differential GTS with Continuous Update

$V_{PROC}$  is directly proportional to the magnetic flux density,  $B$ , induced by the target and sensed by the Hall elements. When  $V_{PROC}$  transitions through a switchpoint from the appropriate higher or lower level, it triggers sensor switch turn-on and turn-off. As shown in figure 3, when the switch is in the off state, as  $V_{PROC}$  rises through a certain limit, referred to as the *operate point*,  $B_{OP}$ , the switch toggles from off to on. When the switch is in the on state, as  $V_{PROC}$  falls below  $B_{OP}$  to a certain limit, the

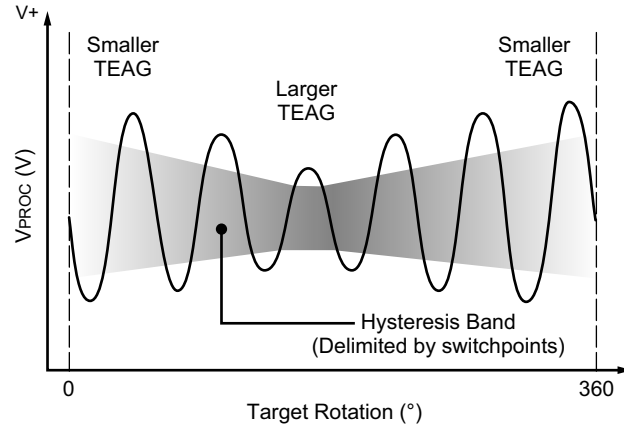
*release point*,  $B_{RP}$ , the switch toggles from on to off.

As shown in panel C of figure 4, threshold levels for the ATS643 switchpoints are established dynamically as function of the peak input signal levels. The ATS643 incorporates an algorithm that continuously monitors the system and updates the switching thresholds accordingly. The switchpoint for each edge is determined by the detection of the previous two edges. In this manner, variations are tracked in real time.

(A) TEAG varying; cases such as eccentric mount, out-of-round region, normal operation position shift



(B) Internal analog signal,  $V_{PROC}$ , typically resulting in the sensor



(C) Referencing the internal analog signal,  $V_{PROC}$ , to continuously update device response

$B_{HYS}$	Switchpoint	Determinant Peak Values
1	$B_{OP}(\#1)$ $B_{RP}(\#1)$	$PK_{(\#1)}$ , $PK_{(\#2)}$ $PK_{(\#2)}$ , $PK_{(\#3)}$
2	$B_{OP}(\#2)$ $B_{RP}(\#2)$	$PK_{(\#3)}$ , $PK_{(\#4)}$ $PK_{(\#4)}$ , $PK_{(\#5)}$
3	$B_{OP}(\#3)$ $B_{RP}(\#3)$	$PK_{(\#5)}$ , $PK_{(\#6)}$ $PK_{(\#6)}$ , $PK_{(\#7)}$
4	$B_{OP}(\#4)$ $B_{RP}(\#4)$	$PK_{(\#7)}$ , $PK_{(\#8)}$ $PK_{(\#8)}$ , $PK_{(\#9)}$

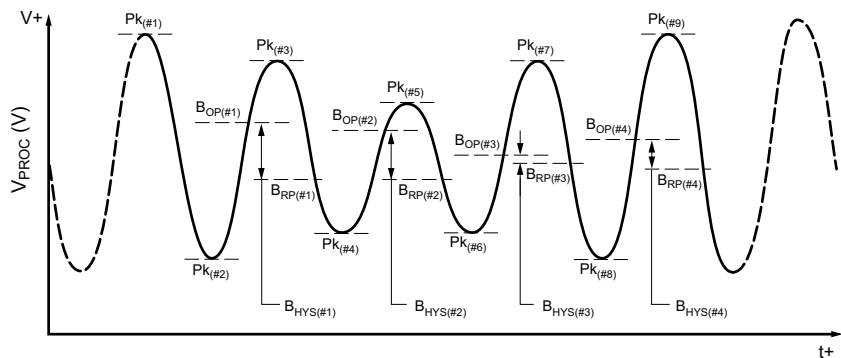


Figure 4. The Continuous Update algorithm allows the Allegro sensor to immediately interpret and adapt to significant variances in the magnetic field generated by the target as a result of eccentric mounting of the target, out-of-round target shape, elevation due to lubricant build-up in journal gears, and similar dynamic application problems that affect the TEAG (Total Effective Air Gap). The algorithm is used to dynamically establish and subsequently update the device switchpoints ( $B_{OP}$  and  $B_{RP}$ ). The hysteresis,  $B_{HYS}(\#x)$ , at each target feature configuration results from this recalibration, ensuring that it remains properly proportioned and centered within the peak-to-peak range of the internal analog signal,  $V_{PROC}$ .

As shown in panel A, the variance in the target position results in a change in the TEAG. This affects the sensor as a varying magnetic field, which results in proportional changes in the internal analog signal,  $V_{PROC}$ , shown in panel B. The Continuous Update algorithm is used to establish accurate switchpoints based on the fluctuation of  $V_{PROC}$ , as shown in panel C.

# ATS643LSH

## Self-Calibrating, Zero-Speed Differential GTS with Continuous Update

**Power-On State Operation.** The ATS643 is guaranteed to power-on in the high current state,  $I_{CC(High)}$ .

**Initial Edge Detection.** The device self-calibrates using the initial teeth sensed, and then enters Running mode. This results in reduced accuracy for a brief period (less than four teeth),

however, it allows the device to optimize for continuous update yielding adaptive sensing during Running mode. As shown in figure 5, the first three high peak signals are used to calibrate AGC. However, there is a slight variance in the duration of initialization, depending on what target feature is nearest the sensor when power-on occurs.

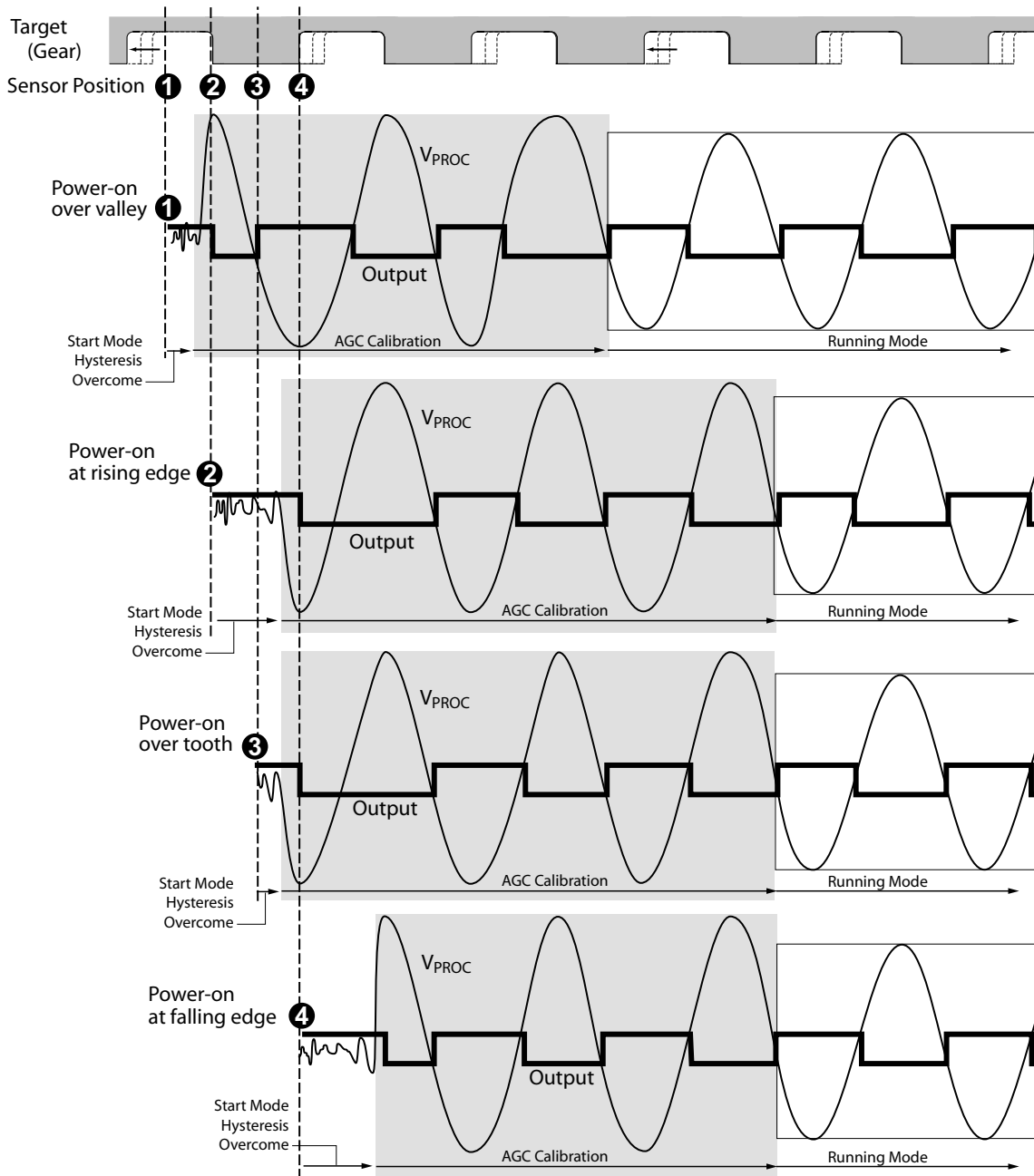


Figure 5. Power-on initial edge detection. This figure demonstrates four typical power-on scenarios. All of these examples assume that the target is moving relative to the sensor in the direction indicated. The length of time required to overcome Start Mode Hysteresis, as well as the combined effect of whether it is overcome in a positive or negative direction plus whether the next edge is in that same or opposite polarity, affect the point in time when AGC calibration begins. Three high peaks are always required for AGC calibration.

# ATS643LSH

## Self-Calibrating, Zero-Speed Differential GTS with Continuous Update

**Start Mode Hysteresis.** This feature helps to ensure optimal self-calibration by rejecting electrical noise and low-amplitude target vibration during initialization. This prevents AGC from calibrating the sensor on such spurious signals. Calibration can be performed using the actual target features.

A typical scenario is shown in figure 6. The hysteresis,  $PO_{HYS}$ , is a minimum level of the peak-to-peak amplitude of the internal analog electrical signal,  $V_{PROC}$ , that must be exceeded before the ATS643 starts to compute switchpoints.

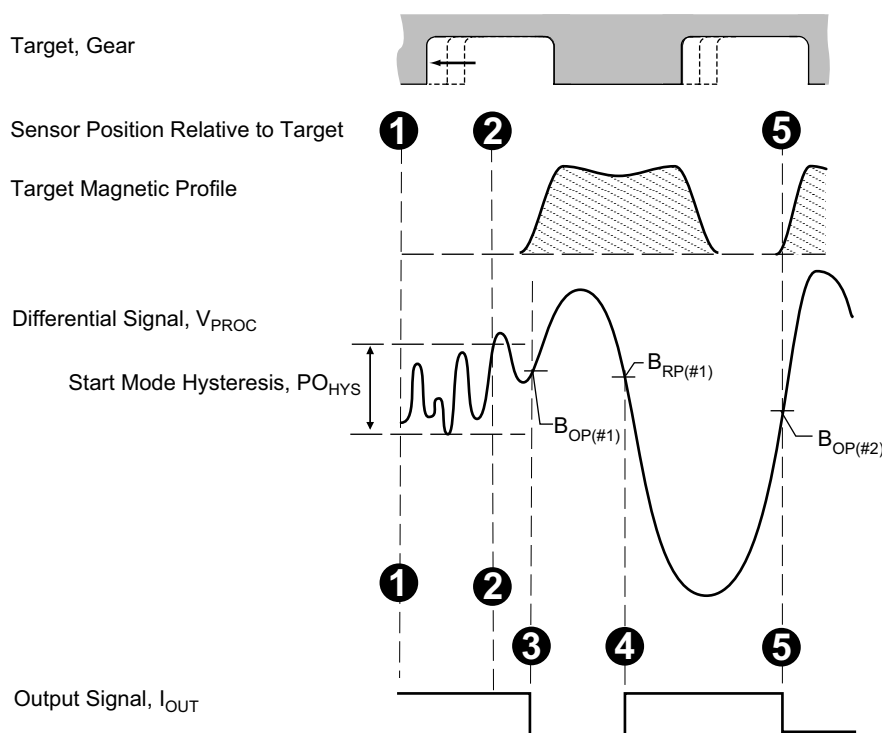


Figure 6. Operation of Start Mode Hysteresis

Position 1. At power-on, the ATS643 begins sampling  $V_{PROC}$ .

Position 2. At the point where the Start Mode Hysteresis is exceeded, the device begins to establish switching thresholds ( $B_{OP}$  and  $B_{RP}$ ) using the Continuous Update algorithm. After this point, Start Mode Hysteresis is no longer a consideration. Note that a valid  $V_{PROC}$  value exceeding the Start Mode Hysteresis can be generated either by a legitimate target feature or by excessive vibration.

Position 3. In this example, the first switchpoint transition is through  $B_{OP}$ , and the output transitions from high to low.

If the first switchpoint transition had been through  $B_{RP}$  (such as position 4), no output transition would occur because  $I_{OUT}$  already would be in the high polarity. The first transition would occur at position 5 ( $B_{OP}$ ).

# ATS643LSH

## Self-Calibrating, Zero-Speed Differential GTS with Continuous Update

**Undervoltage Lockout.** When the supply voltage falls below the minimum operating voltage,  $V_{CC(UV)}$ ,  $I_{CC}$  goes high and remains high regardless of the state of the magnetic gradient from the target. This lockout feature prevents false signals, caused by undervoltage conditions, from propagating to the output of the sensor.

**Power Supply Protection.** The device contains an on-chip regulator and can operate over a wide  $V_{CC}$  range. For devices that need to operate from an unregulated power supply, transient protection must be added externally. For applications using a regulated line, EMI/RFI protection may still be required. Contact Allegro Microsystems for information on the circuitry needed for compliance with various EMC specifications. Refer to figure 7 for an example of a basic application circuit.

**Automatic Gain Control (AGC).** This feature allows the device to operate with an optimal internal electrical signal, regardless of the air gap (within the AG specification). At

power-on, the device determines the peak-to-peak amplitude of the signal generated by the target. The gain of the sensor is then automatically adjusted. Figure 8 illustrates the effect of this feature.

**Automatic Offset Adjust (AOA).** The AOA is patented circuitry that automatically cancels the effects of chip, magnet, and installation offsets. (For capability, see Dynamic Offset Cancellation, in the Operating Characteristics table.) This circuitry is continuously active, including both during power-on mode and running mode, compensating for any offset drift. Continuous operation also allows it to compensate for offsets induced by temperature variations over time.

**Assembly Description.** The ATS643 is integrally molded into a plastic body that has been optimized for size, ease of assembly, and manufacturability. High operating temperature materials are used in all aspects of construction.

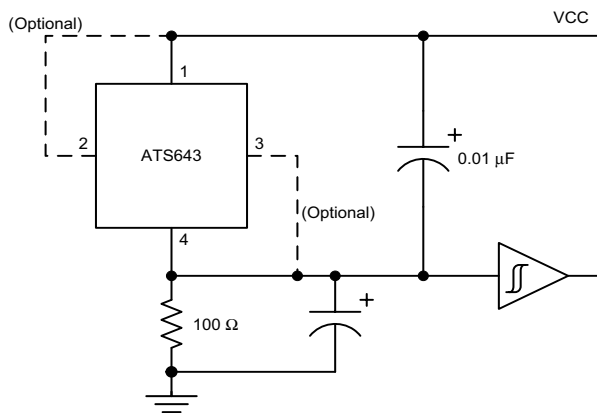


Figure 7. Typical basic circuit for proper device operation.

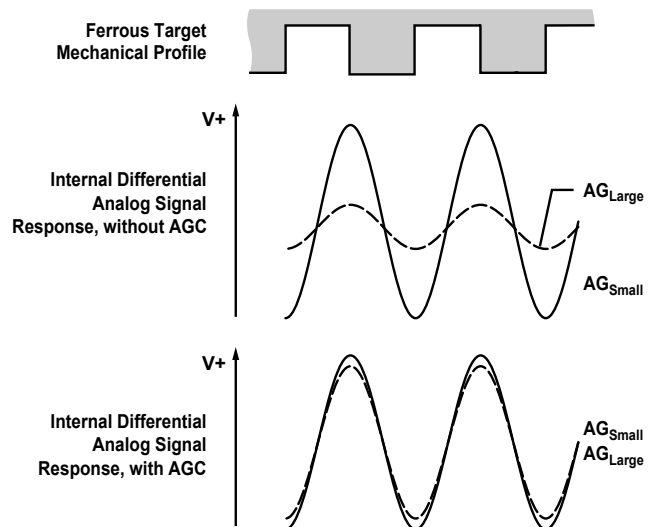


Figure 8. Automatic Gain Control (AGC). The AGC function corrects for variances in the air gap. Differences in the air gap cause differences in the magnetic field at the device, but AGC prevents that from affecting device performance, as shown in the lowest panel.

# ATS643LSH

## Self-Calibrating, Zero-Speed Differential GTS with Continuous Update

### Power Derating

The device must be operated below the maximum junction temperature of the device,  $T_{J(max)}$ . Under certain combinations of peak conditions, reliable operation may require derating supplied power or improving the heat dissipation properties of the application. This section presents a procedure for correlating factors affecting operating  $T_J$ . (Thermal data is also available on the Allegro MicroSystems Web site.)

The Package Thermal Resistance,  $R_{\theta JA}$ , is a figure of merit summarizing the ability of the application and the device to dissipate heat from the junction (die), through all paths to the ambient air. Its primary component is the Effective Thermal Conductivity,  $K$ , of the printed circuit board, including adjacent devices and traces. Radiation from the die through the device case,  $R_{\theta JC}$ , is relatively small component of  $R_{\theta JA}$ . Ambient air temperature,  $T_A$ , and air motion are significant external factors, damped by overmolding.

The effect of varying power levels (Power Dissipation,  $P_D$ ), can be estimated. The following formulas represent the fundamental relationships used to estimate  $T_J$ , at  $P_D$ .

$$P_D = V_{IN} \times I_{IN} \quad (1)$$

$$\Delta T = P_D \times R_{\theta JA} \quad (2)$$

$$T_J = T_A + \Delta T \quad (3)$$

For example, given common conditions such as:  $T_A = 25^\circ\text{C}$ ,  $V_{CC} = 12\text{ V}$ ,  $I_{CC} = 4\text{ mA}$ , and  $R_{\theta JA} = 140^\circ\text{C/W}$ , then:

$$P_D = V_{CC} \times I_{CC} = 12\text{ V} \times 4\text{ mA} = 48\text{ mW}$$

$$\Delta T = P_D \times R_{\theta JA} = 48\text{ mW} \times 140^\circ\text{C/W} = 7^\circ\text{C}$$

$$T_J = T_A + \Delta T = 25^\circ\text{C} + 7^\circ\text{C} = 32^\circ\text{C}$$

A worst-case estimate,  $P_{D(max)}$ , represents the maximum allowable power level ( $V_{CC(max)}$ ,  $I_{CC(max)}$ ), without exceeding  $T_{J(max)}$ , at a selected  $R_{\theta JA}$  and  $T_A$ .

*Example:* Reliability for  $V_{CC}$  at  $T_A = 150^\circ\text{C}$ , package L-II1, using minimum-K PCB

Observe the worst-case ratings for the device, specifically:  $R_{\theta JA} = 126^\circ\text{C/W}$ ,  $T_{J(max)} = 165^\circ\text{C}$ ,  $V_{CC(max)} = 24\text{ V}$ , and  $I_{CC(max)} = 16\text{ mA}$ .

Calculate the maximum allowable power level,  $P_{D(max)}$ . First, invert equation 3:

$$\Delta T_{max} = T_{J(max)} - T_A = 165^\circ\text{C} - 150^\circ\text{C} = 15^\circ\text{C}$$

This provides the allowable increase to  $T_J$  resulting from internal power dissipation. Then, invert equation 2:

$$P_{D(max)} = \Delta T_{max} \div R_{\theta JA} = 15^\circ\text{C} \div 126^\circ\text{C/W} = 119\text{ mW}$$

Finally, invert equation 1 with respect to voltage:

$$V_{CC(est)} = P_{D(max)} \div I_{CC(max)} = 119\text{ mW} \div 16\text{ mA} = 7\text{ V}$$

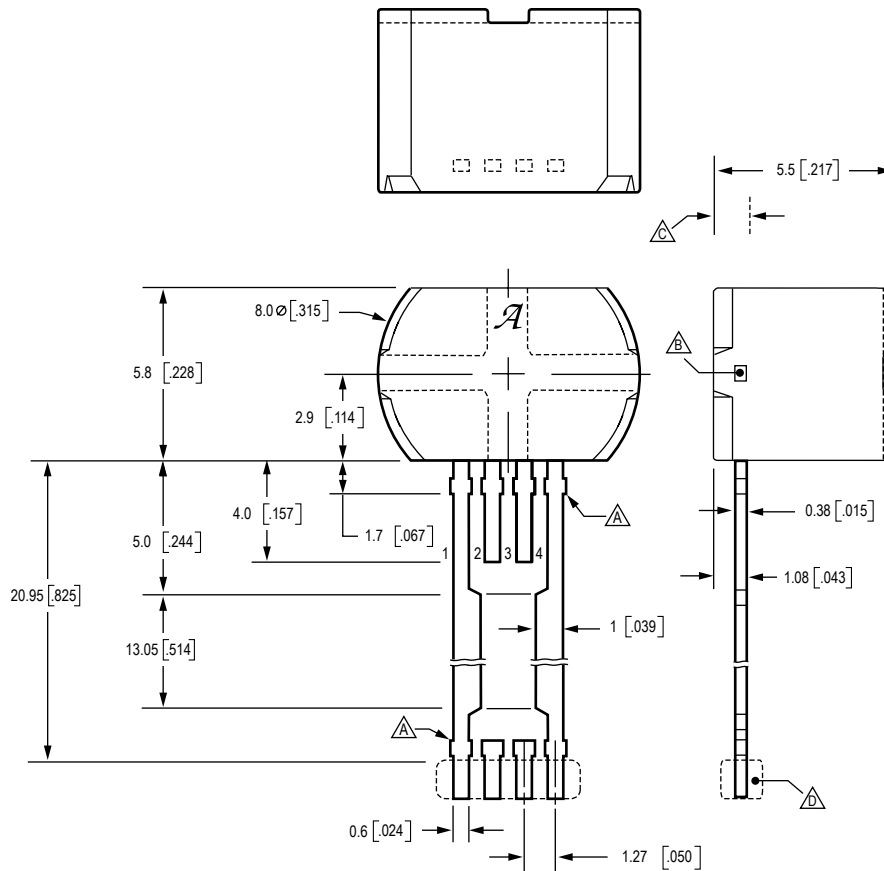
The result indicates that, at  $T_A$ , the application and device can dissipate adequate amounts of heat at voltages  $\leq V_{CC(est)}$ .

Compare  $V_{CC(est)}$  to  $V_{CC(max)}$ . If  $V_{CC(est)} \leq V_{CC(max)}$ , then reliable operation between  $V_{CC(est)}$  and  $V_{CC(max)}$  requires enhanced  $R_{\theta JA}$ . If  $V_{CC(est)} \geq V_{CC(max)}$ , then operation between  $V_{CC(est)}$  and  $V_{CC(max)}$  is reliable under these conditions.

# ATS643LSH

Self-Calibrating, Zero-Speed Differential GTS with Continuous Update

Package SH, 4-pin SIP



- Dimensions in millimeters. Untoleranced dimensions are nominal.  
U.S. Customary dimensions (in.) in brackets, for reference only
- Dambar removal protrusion
  - Metallic protrusion, electrically connected to pin 4 and substrate (both sides)
  - Active Area Depth 0.43 mm [.017]
  - Thermoplastic Molded Lead Bar for alignment during shipment

# ATS643LSH

## Self-Calibrating, Zero-Speed Differential GTS with Continuous Update

*The products described herein are manufactured under one or more of the following U.S. patents: 5,045,920; 5,264,783; 5,442,283; 5,389,889; 5,581,179; 5,517,112; 5,619,137; 5,621,319; 5,650,719; 5,686,894; 5,694,038; 5,729,130; 5,917,320; and other patents pending.*

*Allegro MicroSystems, Inc. reserves the right to make, from time to time, such departures from the detail specifications as may be required to permit improvements in the performance, reliability, or manufacturability of its products. Before placing an order, the user is cautioned to verify that the information being relied upon is current.*

*Allegro products are not authorized for use as critical components in life-support devices or systems without express written approval.*

*The information included herein is believed to be accurate and reliable. However, Allegro MicroSystems, Inc. assumes no responsibility for its use; nor for any infringement of patents or other rights of third parties which may result from its use.*

Copyright © 2004 Allegro MicroSystems, Inc.